Walisongo Journal of Chemistry
Walisongo Journal of Chemistry Vol. 8 Issue 2 (2025), 306-316
ISSN: 2621-5985 (online); 2549-385X (print)
DOI: https://doi.org/10.21580/wjc.v8i2.28937

INORGANIC OXIDE SYNTHESIS FROM ACEH BOVINE BONE USING THE PRECIPITATION METHOD FOR BIOMASS TRANSESTERIFICATION

Nisa Amlia[1], Muliadi Ramli[1], Ratu Balqis Rossani[1], Rara Mitaphonna[2], Surya Lubis[1], Nasrullah Idris[3], Saiful[1], Fathurrahmi[1]

[1]Department of Chemistry, Faculty of Mathematics and Natural Sciences, Universitas Syiah Kuala, Banda Aceh,23115
[2]Research Center for Photonic, National Research and Innovation Agency (BRIN), Tangerang Selatan 15314, Indonesia
[3] Department of Physics, Faculty of Mathematics and Natural Sciences, Universitas Syiah Kuala, Banda Aceh, Indonesia, 23115

*Corresponding author: muliadiramli@usk.ac.id

Abstract

Inorganic oxide nanoparticles synthesized from Aceh bovine bone were successfully prepared using the precipitation method, with pH variations of 8 and 10 adjusted using NH_4OH as the precipitating agent and pH regulator. The resulting nanocatalysts were characterized using XRD, FTIR, and SEM-EDX, and their catalytic activity was evaluated through the transesterification of RBDPO. XRD and FTIR analyses confirmed the presence of hydroxyapatite ($Ca_{10}(PO_4)_6(OH)_2$), calcium oxide (CaO), and calcium carbonate ($CaCO_3$) as the main components in catalysts synthesized at pH 8 and pH 10. SEM micrographs revealed spherical particle morphologies, while EDX analysis showed calcium as the dominant element, with contents of 55.44% and 57.19%, respectively. The average crystallite sizes, calculated using the Debye–Scherrer equation, were 31.63 nm (CB-P8C) and 31.31 nm (CB-P10C). Catalytic activity tests demonstrated that the catalyst synthesized at pH 10 exhibited higher performance, achieving a biodiesel yield of 98.11%, compared to 92.66% for the catalyst synthesized at pH 8. Quality assessment of both biodiesel samples confirmed that their acid values, density, and viscosity met the Indonesian National Standard (SNI 04-7182-2015). This approach highlights a sustainable pathway for converting biowaste into efficient catalysts for green fuel production.

Keywords: *nanocatalyst, inorganic oxide, bovine bone, biodiesel*

Introduction

The growth of the global population and economy, including in Indonesia, has increased fossil fuel consumption for diesel engines (Hussein & Idris, 2024). Biodiesel has emerged as a prominent alternative energy source, accounting for 82% of global biofuel production and serving as a key solution to meet future energy demands in residential and industrial sectors (Naseef & Tulaimat, 2025). Indonesia and the United States are the largest biodiesel producers worldwide, with outputs of 7.9 and 6.5

billion liters, respectively, in 2019. It is projected that biodiesel could replace up to 7% of global fossil fuel consumption by 2030 (Osman et al., 2024). In addition to being renewable, biodiesel is considered a clean fuel, as it reduces CO, CO_2, CnHn, and particulate matter emissions compared to conventional hydrocarbon-based diesel fuels (Elgharbawy et al., 2021).

The use of heterogeneous catalysts in biodiesel synthesis is preferred due to their ease of separation after the reaction. Among these catalysts, CaO is widely utilized. CaO is an inorganic compound with strong basicity, making it highly effective in various chemical reactions, including transesterification, gas reforming, and organic compound decomposition. The main advantages of CaO as a catalyst include its abundant availability, relatively low cost, and environmental friendliness. CaO can be derived from natural resources such as limestone and dolomite, as well as from the calcination of shells and animal bones (Mazaheri et al., 2021). Various animal bones, including chicken, goat, cattle, pig, fish, bird, and camel, have been reported as effective sources of CaO catalysts for biodiesel transesterification reactions (Hussain et al., 2021).

However, transesterification reactions using CaO-based heterogeneous catalysts present several limitations, including relatively long reaction times and low surface area. These limitations require larger amounts of CaO to achieve satisfactory conversion rates, consequently increasing production costs. To address these challenges, extensive scientific research has focused on improving the catalytic performance of inorganic CaO-based catalysts, particularly by enhancing their efficiency in transesterification reactions. One key strategy is increasing the catalyst's surface area, which can be achieved by synthesizing catalysts with smaller particle sizes. Nanoscale catalysts offer a higher surface-to-volume ratio, providing more active sites and improving catalytic efficiency. Among the available synthesis techniques, the precipitation method has gained popularity for producing nanosized solid catalysts due to its simplicity, cost-effectiveness, and ability to yield uniform nanoparticles (Putri et al., 2024). The precipitation method involves the controlled formation of solid particles from a solution, often facilitated by precipitating agents such as sodium hydroxide (NaOH) (Sunardi et al., 2020), potassium hydroxide (KOH), and ammonium hydroxide (NH_4OH) (Safitri & Puryanti, 2020). These agents play a crucial role in determining the particle size, morphology, and crystallinity of the resulting catalyst, directly influencing its catalytic properties. By optimizing synthesis parameters such as pH, temperature, and the concentration of precipitating agents, researchers aim to tailor the physicochemical characteristics of CaO catalysts to maximize their performance in biodiesel production.

Despite numerous studies on CaO catalysts derived from animal bones, limited research has examined the use of Aceh bovine bone as a precursor material. Aceh, a region in Indonesia with a large cattle farming industry, generates substantial amounts of unused bovine bone waste from slaughterhouses and meat-processing facilities. These bones are typically discarded, leading to environmental and sanitary concerns. Preliminary compositional analyses have shown that Aceh bovine bones are rich in calcium and phosphate minerals with naturally high crystallinity, making them a promising raw material for producing CaO- and hydroxyapatite-based nanocatalysts (Ramli et al., 2020). Utilizing Aceh bovine bone not only adds value to local biowaste but also supports the circular economy and regional sustainability goals by converting agricultural waste into green catalysts.

Therefore, this study aimed to synthesize and characterize inorganic oxide nanocatalysts derived from Aceh bovine bone using the precipitation method under varying pH conditions (8 and 10), and to evaluate their catalytic performance in biodiesel production from refined, bleached, and deodorized palm oil (RBDPO). This work contributes to the development of

sustainable, locally sourced nanocatalysts, offering a novel approach that integrates waste valorization with green energy production.

Experimental Section

Materials

The materials used in this study included local Aceh bovine bone, RBDPO sourced from PT Jhonlin Agro Raya, technical-grade methanol from Smart Lab, NH_4OH, HCl, and KOH (Merck), as well as phenolphthalein (PP) indicator from Smart Lab.

Instruments

The instruments employed in this study included a PANalytical X'Pert PRO X-ray Diffractometer (XRD), a Thermo Nicolet 6700 Fourier Transform Infrared (FTIR) spectrometer, an FEI Inspect S50 Scanning Electron Microscope equipped with Energy Dispersive X-ray Spectroscopy (SEM-EDX), and a Thermo Scientific ISQ 7000 Gas Chromatography–Mass Spectrometry (GC-MS) system.

Procedure

Heterogeneous Catalyst Preparation

The bovine bones were cleaned, washed, and dried in an oven at 110°C for 4 hours. The dried bones were then crushed and sieved using a 100-mesh sieve to obtain a homogeneous bone powder with an average particle size of 150 µm. A 12.5 g portion of the bone powder was weighed and extracted in 250 mL of 2 M HCl at room temperature for 4 hours with continuous stirring using a magnetic stirrer. The resulting extract was filtered to obtain a clear filtrate. Precipitation was performed by gradually adding 5 M NH_4OH solution dropwise into the filtrate until a precipitate was formed, following the method of Sunardi et al. (2020), with pH variations of 8 and 10. The mixture was allowed to stand for 24 hours to ensure complete precipitation. The precipitate was separated and washed with deionized water, weighed, and then dried in an oven at 120°C for 4 hours. Calcination was subsequently conducted in a furnace at 900°C for 4 hours. The resulting inorganic oxide crystals were stored in sealed containers and designated as follows: inorganic oxide catalyst from precipitation at pH 8 (CB-P8), calcined catalyst from precipitation at pH 8 (CB-P8C), inorganic oxide catalyst from precipitation at pH 10 (CB-P10), and calcined catalyst from precipitation at pH 10 (CB-P10C).

Catalyst Characterization

The catalysts were characterized for their physicochemical properties using several analytical techniques. FTIR analysis was employed to identify functional groups based on the chemical bonds present in the samples. XRD analysis was used to determine crystallinity, phase composition, and the compounds formed. SEM-EDX analysis was conducted to observe morphology, elemental composition, and the percentage distribution of each element in the material.

Oil Quality Test

Acid value determination

A total of 10 mL of oil was placed into an Erlenmeyer flask, and three drops of phenolphthalein indicator were added. The mixture was titrated with 0.1 M standard KOH solution until a persistent pink endpoint was reached. The acid value was calculated using the following equation 1.

$$\text{Acid Value} = \frac{\text{Volume of KOH (mL)} \times \text{Concentration of KOH (M)} \times \text{Molecular weight of KOH}}{\text{Mass (g)}} \quad \text{Eq.1}$$

Density determination

The density of the oil was determined using a pycnometer by measuring the mass of the empty pycnometer and the mass of the pycnometer filled with 5 mL of oil. Density was calculated using the following equation 2.

$$\text{Density} = \frac{\text{Mass of the pycnometer with oil (g)} - \text{Mass of the empty pycnometer (g)}}{\text{Volume of Oil (mL)}} \quad \text{Eq 2.}$$

Viscosity determination

The viscosity of the oil was measured using a digital viscometer. The spindle was attached and adjusted so that the sample covered the marked immersion level. The instrument was operated until a stable viscosity reading was obtained.

Biodiesel Synthesis

Biodiesel was synthesized through a transesterification reaction. RBDPO was placed into a three-neck flask with a methanol-to-oil molar ratio of 9:1 and a catalyst loading of 5% (w/w), as reported by Mengistu & Reshad, (2022). The catalyst was preheated at 120°C for 3 hours in an oven to activate it prior to use. The catalyst was added to the three-neck flask equipped with a reflux condenser, magnetic stirrer, and thermometer. The reaction was conducted at 65°C for 4 hours. After completion, the mixture was cooled to room temperature, transferred to a separatory funnel, and allowed to settle for 24 hours. Two layers formed: the upper methyl ester (biodiesel) layer and the lower glycerol layer. The biodiesel composition was analyzed using GC-MS. The yield was calculated using the following Equation 3.

$$\text{Yield} = \frac{\text{Biodiesel mass (g)}}{\text{RBDPO mass (g)}} \; x\; 100\% \quad \text{Eq 3.}$$

The acid value, viscosity, and density of the produced biodiesel were then compared with the SNI 04-7182-2015 standard.

Results and Discussion

Heterogeneous Catalyst Preparation

The preparation of bovine bone followed the procedure reported by Sunardi et al. (2020). The reaction mechanisms involved in the catalyst preparation from the bovine bone powder precursor are shown in Equations (1), (2), and (3). After calcination at 900°C, the catalysts CB-P8C and CB-P10C exhibited a color change to white (see **Figure 1**).

$$CaCO_3(s) + 2HCl(aq) \rightarrow CaCl_2(aq) + H_2O(l) + CO_2(g) \quad (1)$$
$$CaCl_2(aq) + 2NH_4OH(aq) \rightarrow Ca(OH)_2(s) + 2NH_4Cl(aq) \quad (2)$$
$$Ca(OH)_2(s)\ \text{Heated} \rightarrow CaO(s) + H_2O(g) \quad (3)$$

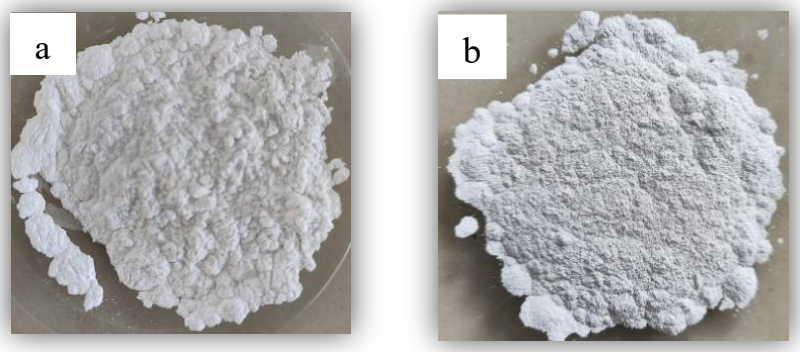

Figure 1. Catalyst images: (a) CB-P8C and (b) CB-P10C.

Catalyst Characterization

XRD

The XRD patterns of the catalyst samples obtained via precipitation before and after calcination at pH 8 and pH 10 are presented in **Figure 2** and **Figure 3**. The results indicate the presence of major compounds typically found in bovine bone, including $Ca_{10}(PO_4)_6(OH)_2$, $CaCO_3$, and $Ca(OH)_2$. Before calcination, the diffractograms of both samples showed characteristic hydroxyapatite peaks at 2θ values of 22.88°, 25.86°, 28.10°, 32.15°, 32.84°, 39.72°, 46.62°, and 49.42°, as well as 25.91°, 28.10°, 32.05°, 39.55°, 46.79°, and 49.65°, consistent with JCPDS card no. 96-900-2215. $CaCO_3$ was identified by peaks near 2θ ≈ 10° and 53°, while $Ca(OH)_2$ was detected at 2θ values of 33°, 58°, and 64° (see **Figure 2**) (Andas & Jusoh, 2022).

The diffraction patterns of the catalysts precipitated at pH 8 and pH 10 after calcination also confirmed the presence of hydroxyapatite, $CaCO_3$, and CaO. Peaks corresponding to hydroxyapatite appeared at 16.83°, 25.75°, 27.96°, 31.79°, 32.15°, 39.12°, and 49.42° (JCPDS 96-901-7412), as well as 16.82°, 25.92°, 28.10°, 31.72°, 32.15°, 39.14°, and 49.42° (JCPDS 96-101-1243). Calcium carbonate was confirmed by peaks at 34.55° and 46.26° (JCPDS 96-901-7412) and at 34.55° and 45.93° (JCPDS 96-901-7415). Peaks at 64.16° and 64.15° correspond to CaO, consistent with JCPDS 96-900-6746. The CaO detected in the calcined catalysts is formed through the thermal decomposition of $Ca(OH)_2$ and $CaCO_3$. This phenomenon has also been reported by Khan et al. (2020), who noted that $CaCO_3$ readily decomposes to CaO in the presence of oxygen.

A clear difference was observed between the catalysts synthesized at pH 8 and pH 10. The XRD peaks of the pH 10 catalyst were sharper and more intense, indicating higher crystallinity and improved structural ordering compared to the pH 8 catalyst. This suggests that precipitation at higher pH promotes more complete hydroxide formation and controlled nucleation, enhancing the conversion of $Ca(OH)_2$ and $CaCO_3$ into CaO during calcination. Catalysts prepared under higher pH conditions also tend to exhibit smaller particle sizes and larger surface areas, increasing the number of accessible active sites and improving catalytic efficiency. Therefore, the higher crystallinity of the pH 10 catalyst is expected to enhance its catalytic performance by providing more well-defined and reactive surface sites for the transesterification reaction. In contrast, the broader peaks in the pH 8 catalyst indicate smaller and less ordered crystallites, which may reduce catalytic activity (Permanasari et al., 2022).

Crystallite sizes calculated using the Debye–Scherrer equation yielded average values of 31.63 nm (CB-P8C) and 31.31 nm (CB-P10C). These nanoscale dimensions (<100 nm) are consistent with the findings of Sunardi et al. (2020), who also reported crystallite sizes within the nanometer range.

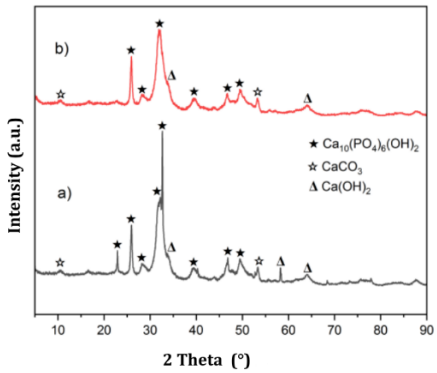

Figure 2. XRD diffractograms for (a) CB-P8 and (b) CB-P10.

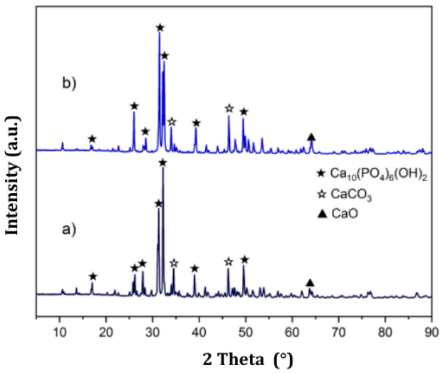

Figure 3. XRD diffractograms for (a) CB-P8C and (b) CB-P10C.

Copyright © 2025 WJC | ISSN 2621-5985 (online) | ISSN 2549-385X (print)
Volume 8, Nomor 2, 2025

FTIR

The FTIR spectra of the inorganic oxide catalysts obtained via precipitation at pH 8 and pH 10, as well as those calcined at 900°C for 4 h, are shown in **Figure 4**. All four catalysts exhibited similar absorption bands. The absorption bands at 3416.12 cm^{-1}, 3436.33 cm^{-1}, 3416.08 cm^{-1}, and 3558.82 cm^{-1} correspond to hydroxyl (–OH) groups, with sharper peaks observed after calcination. Previous studies on bovine-bone-derived catalysts also reported –OH vibrations around 3400–3500 cm^{-1} (Chukwuemeke et al., 2023; Hassan & Fadhil, 2021).

In addition to –OH groups, all spectra displayed absorption bands associated with carbonate (CO_3^{2-}) and phosphate (PO_4^{3-}) groups. Carbonate groups were detected in the 1408–1467 cm^{-1} region, while phosphate groups appeared between 1035–1039 cm^{-1}. Minor shifts in these bands among samples indicate structural changes or variations in bonding caused by calcination. Absorption bands in the 565–575 cm^{-1} range correspond to Ca–O vibrations formed after calcination. Bands within 600–400 cm^{-1} in bovine bone FTIR spectra are generally attributed to Ca–O bond vibrations induced by heat treatment (Khan et al., 2020). Overall, the FTIR results confirm that the catalysts CB-P8, CB-P10, CB-P8C, and CB-P10C contain hydroxyapatite ($Ca_{10}(PO_4)_6(OH)_2$) (Hassan & Fadhil, 2021).

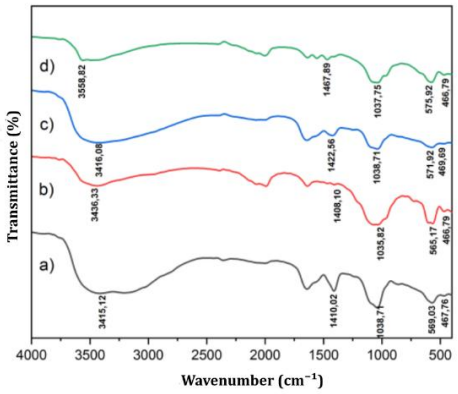

Figure 4. FTIR spectra for (a) CB-P8, (b) CB-P8C, (c) CB-P10, and (d) CB-P10C.

SEM-EDX

The characterization results obtained from Scanning Electron Microscopy (SEM) at 20,000× magnification, along with the particle size distribution histograms, are presented in **Figure 5**. The SEM images of bovine bone catalysts precipitated at pH 8 and 10 before calcination reveal irregular (amorphous) aggregates and agglomerates. The formation of amorphous particles aligns with the findings reported by Prayitno et al. (2020), who stated that following the nucleation process, the formation of the smallest stable units of a new phase under precipitation conditions, the subsequent growth phase occurs. Under high supersaturation conditions, the nucleation rate significantly exceeds the crystal growth rate, leading to the formation of numerous small particles and resulting in amorphous precipitate material.

The surface morphology of the catalyst particles precipitated at pH 8 after calcination (see **Figure 5c**) exhibited spherical shapes resembling stacked and fused balls, with a noticeable reduction in agglomeration. Although the spherical morphology was not clearly visible in all SEM images, the overall structure could still be inferred from the general particle shapes and their behavior during synthesis using the precipitation method. As shown in **Figure 5(e)**, a similar morphology was observed, although with smaller particle sizes. Amri et al. (2024), who synthesized Blood Clam Shells using the precipitation method, also observed that the resulting CaO particles exhibited spherical, ball-like structures. This transformation occurred because the irregular (amorphous) aggregates were converted into more defined and homogeneous particles following thermal decomposition during calcination at 900°C. These observations indicate that the precipitation process enhances the crystalline structure of nano-sized calcium oxide, producing a more ordered and uniform catalyst than non-precipitated catalysts (Adji et al., 2023).

Variation in catalyst particle size with respect to pH was attributed to

differences in the nucleation and crystal growth phases during precipitation, which proceeded more optimally at the higher pH of 10 than at pH 8 (Safitri & Puryanti, 2020). This finding is consistent with the crystallite size calculations obtained using the Debye–Scherrer equation. It was further supported by ImageJ analysis, which showed average particle sizes of 94 nm for pH 8 and 81 nm for pH 10, both of which fell within the nanometer scale (see **Figure 5d** and **Figure 5f**). These results are also consistent with similar elements, with Ca being the highest at 47.95%. After calcination, the Ca percentage increased to 55.44% and 57.19% (Shabani & Faraji, 2020). The EDX data presented in **Table 2** correlate with the XRD diffractogram data (see **Figure 2** and **Figure 3**) and FTIR spectra (see **Figure 4**), which confirm the presence of $Ca_{10}(PO_4)_6(OH)_2$ in all characterized catalysts.

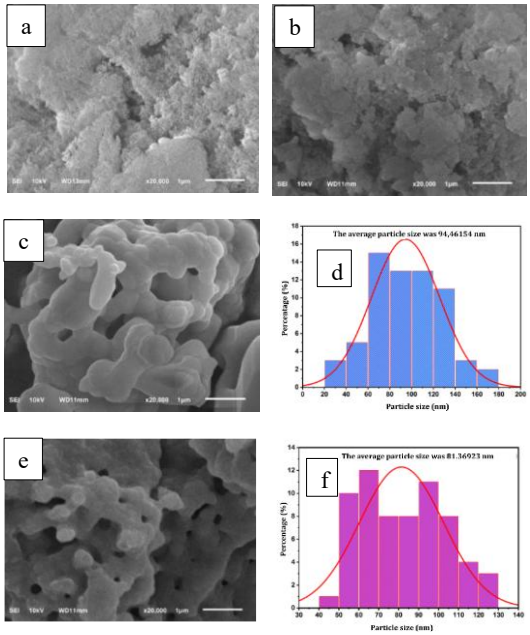

Figure 5. SEM images of (a) CB-P8, (b) CB-P10, (c) CB-P8C, and (d) CB-P10C; (e) particle size distribution histogram for CB-P8C; (f) particle size distribution histogram for CB-P10C.

Biodiesel Synthesis

The transesterification reaction was conducted using an RBDPO-to-methanol findings reported by Sunardi et al. (2020), who observed nanoscale particle sizes in calcium oxide catalysts synthesized via precipitation.

Several elements present in the four catalyst samples were analyzed using EDX, as shown in **Table 1**. For the inorganic precipitated catalyst at pH 8, the dominant element was Ca, accounting for 41.70%, followed by C, P, O, and Cl (Ghifari & Samik, 2023). Meanwhile, the inorganic precipitated catalyst at pH 10 also contained molar ratio of 1:9 at 65°C for 4 hours, and the resulting biodiesel yield is presented in **Figure 6**. The GC–MS chromatogram of the CB-P8C catalyst showed a total methyl ester content of 83.8% (see **Table 2**), with identified FAMEs including methyl oleate (34.04%), methyl palmitate (28.96%), methyl linoleate (8.01%), methyl myristate (7.78%), and methyl stearate (5.01%). Meanwhile, the GC–MS chromatogram for the CB-P10C catalyst indicated a total methyl ester content of 84.1%.

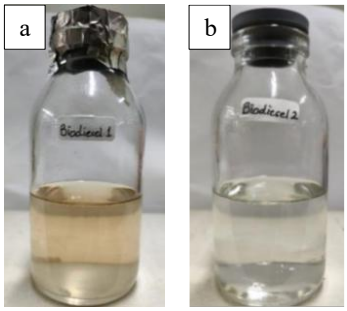

Figure 6. Biodiesel produced from the transesterification of RBDPO with methanol using catalysts (a) CB-P8 and (b) CB-P10.

The GC–MS chromatogram of biodiesel synthesized using the calcined precipitated catalyst at pH 10, shown in **Table 3**, also revealed a total methyl ester content of 84.1%. The individual methyl ester components included methyl laurate (35.76%), methyl myristate (19.01%), methyl palmitate (12.97%), methyl oleate (12.23%), methyl stearate (3.16%), and methyl linoleate (0.97%).

Table 1. EDX analysis data of the characterized catalysts

Elemental Composition (%)	Value			
	CB-P8	CB-P10	CB-P8C	CB-P10C
O K	11.76	7.43	4.17	7.19
P K	19.74	21.80	23.88	23.90
Ca K	41.70	47.95	55.44	57.19
Cl K	3.59	3.36	4.73	4.64
C K	22.14	18.99	10.64	5.67
Mg K	0.44	0.14	0.40	0.59
Mn K	0.33	0.33	0.34	0.35
Fe K	0.30	-	0.40	0.46

Table 2. Composition and Percentage of FAME from Transesterification Using CB-P8C

Retention Time (min)	Area (%)	FAME Composition
31.719	28.96	Methyl palmitate
35.022	34.04	Methyl oleate
34.910	8.01	Methyl linoleate
27.590	7.78	Methyl myristate
35.491	5.01	Methyl stearate

Table 3. Composition and Percentage of FAME from Transesterification Using CB-P10C

Retention Time (min)	Area (%)	FAME Composition
23.043	35.76	Methyl laurate
27.587	19.01	Methyl myristate
31.719	12.97	Methyl palmitate
35.015	12.23	Methyl oleate
35.488	3.16	Methyl stearate
34.910	0.97	Methyl linoleate

In contrast to the biodiesel produced using the catalyst precipitated at pH 8, which was predominantly composed of methyl oleate, the biodiesel produced with the catalyst precipitated at pH 10 showed methyl laurate as its major component. Notably, methyl laurate was not detected in the biodiesel synthesized using the pH 8 catalyst. The higher yield and distinct compositional profile obtained with the pH 10 catalyst can be attributed to its enhanced physicochemical characteristics. The larger surface area and smaller crystallite size of the pH 10 catalyst provide more accessible active sites, thus promoting the formation of shorter-chain methyl esters such as methyl laurate. These structural advantages accelerate reaction kinetics and contribute to a higher overall biodiesel yield compared to the pH 8 catalyst (Kingkam et al., 2024). Although catalyst reusability was not investigated in this study, CaO-based catalysts are generally susceptible to gradual deactivation due to surface carbonation and moisture absorption. Future studies should evaluate catalyst recovery and regeneration over multiple reaction cycles to determine suitability for long-term industrial applications.

Biodiesel Quality Test

After the biodiesel was produced, the yield was determined by comparing the mass of the biodiesel obtained with the initial mass of RBDPO used as feedstock. The results, presented in **Table 4**, show that Biodiesel A achieved a yield of 92.66%, while Biodiesel B reached 98.11%. The higher yield of Biodiesel B aligns with the GC–MS chromatogram findings. The yields obtained in this study were higher than those reported by Mengistu & Reshad, (2022), who employed a similar methanol-to-oil ratio of 9:1 and a catalyst concentration of 5%. Based on the biodiesel quality test, which included acid number, density, and viscosity, all parameters met the quality requirements specified in the Indonesian Biodiesel Standard (SNI 7182:2015), as shown in **Table 4**.

Table 4. Biodiesel yield percentage and quality test results

Parameter	Value			SNI
	RBDPO	CB-P8C (A)	CB-P810 (B)	
Yield (%)	-	92.66	98.11	-
Acid number (mg KOH/g)	0.78945	0.477843	0.436065	Max 0.5
Density (g/mL)	0.93894	0.8568	0.86412	0.85-0.9
Viscosity (cSt)	42.9	3.151261	3.934639	2.3-6.0

Conclusion

This study confirmed the successful synthesis of inorganic catalysts derived from bovine bone using the precipitation method at pH 8 and 10, with and without calcination. XRD and FTIR analyses identified hydroxyapatite, CaO, and $CaCO_3$ as the primary components, while particle size measurements (Debye–Scherrer ≈ 31 nm; SEM 81–94 nm) verified the formation of nanocatalysts. SEM and EDX results indicated a morphological transformation into spherical structures after calcination at 900°C, with Ca, C, O, and P detected as the dominant elements. The calcined pH 10 catalyst produced the highest biodiesel yield (98.11%), outperforming the calcined pH 8 catalyst (92.66%). Both catalysts met the SNI 7182:2015 standards, demonstrating their potential as eco-friendly materials for high-quality biodiesel production. However, this study did not assess catalyst reusability, long-term stability, or scale-up performance. Future research should examine catalyst durability across multiple reaction cycles and evaluate the feasibility of large-scale biodiesel synthesis using this biowaste-derived nanocatalyst.

Acknowledgment

This experiment was funded by Universitas Syiah Kuala (USK), Banda Aceh, Indonesia through a Professor's Research Scheme under the Grant-in-Aid Contract No. 314314/UN11.LI/PG.01.03/14557-PTNBH/2025

References

Adji, N. T. L., Lucytasari, S. D., & Suprihatin, S. (2023). Sintesis dan karakterisasi nanokalsium oksida dari cangkang kerang hijau dengan metode presipitasi. *Jurnal Teknik Kimia*, *18*(1), 65–69 . https://doi.org/10.33005/jurnal_tekkim.v18i1.4127

Amri, A. A., Shorea, Z., & Astuti, C. P. (2024). Synthesis and characterization of nanoparticle calcium oxide (CaO) from blood calm shell by precipitation methods. *Advance Sustainable Science, Engineering and Technology*, *6*(4), 1–8. https://doi.org/10.26877/asset.v6i4.765

Andas, J., & Jusoh, N. F. E. (2022). Converting waste chicken bones into heterogeneous catalyst for biodiesel synthesis from waste cooking oil. *Malaysian Journal of Analytical Sciences*, *26*(5), 1102–1111. 10.17576/jsm-2025-5402-15.

Chukwuemeke, U. W., Eyankware, U. O. R., & Egwunyenga, M. C. (2023). Investigation of the potential of waste bones as a catalyst in biofuel production. *Journal of Wastes and Biomass Management*, *5*(1), 15–21. https://doi.org/10.26480/jwbm.01.2023.15.21

Elgharbawy, A. S., Sadik, W. A., Sadek, O. M., & Kasaby, M. A. (2021). A review on biodiesel feedstocks and production technologies. *Journal of the Chilean Chemical Society*, *66*(1), 5098–5109. https://doi.org/10.4067/S071797072021000105098.

Ghifari, M. I. Al, & Samik, dan S. (2023). Review: Production of biodiesel with transesterification method using catalyst made from waste bone. *UNESA Journal of Chemistry*, *12*(1), 1–11.

Hassan, M. M., & Fadhil, A. B. (2021). Development of an effective solid base catalyst from potassium based chicken

bone (K-CBs) composite for biodiesel production from a mixture of non-edible feedstocks. *Energy Sources, Part A: Recovery, Utilization and Environmental Effects*, *2*, 1–16. https://doi.org/10.1080/15567036.2021.1927253

Hussain, F., Alshahrani, S., Abbas, M. M., Khan, H. M., Jamil, A., Yaqoob, H., Soudagar, M. E. M., Imran, M., Ahmad, M., & Munir, M. (2021). Review waste animal bones as catalysts for biodiesel production; a mini review. *Catalysts*, *11*(5), 1–15. https://doi.org/10.3390/catal11050630

Hussein, M., & Idris, M. (2024). Studi eksperimental titik nyala dan viskositas biodiesel diproduksi dari minyak goreng bekas. *IRA Jurnal Teknik Mesin dan Aplikasinya (IRAJTMA)*, *3*(1), 86–92. https://doi.org/10.56862/irajtma.v3i1.101

Khan, H. M., Iqbal, T., Ali, C. H., Javaid, A., & Cheema, I. I. (2020). Sustainable biodiesel production from waste cooking oil utilizing waste ostrich (Struthio camelus) bones derived heterogeneous catalyst. *Fuel*, *277*, 1–10. https://doi.org/10.1016/j.fuel.2020.118091

Kingkam, W., Maisomboon, J., Khamenkit, K., Nuchdang, S., Nilgumhang, K., Issarapanacheewin, S., & Rattanaphra, D. (2024). Preparation of CaO@CeO2 solid base catalysts used for biodiesel production. *Catalysts*, *14*(240), 1–15. https://doi.org/10.3390/catal14040240

Mazaheri, H., Ong, H. C., Amini, Z., Masjuki, H. H., Mofijur, M., Su, C. H., Badruddin, I. A., & Yunus Khan, T. M. (2021). An overview of biodiesel production via calcium oxide based catalysts: Current state and perspective. *Energies*, *14*(13), 1–23. https://doi.org/10.3390/en14133950

Mengistu, T. G., & Reshad, S. A. (2022). Synthesis and characterization of a heterogeneous catalyst from a mixture of waste animal teeth and bone for castor seed oil biodiesel production. *Heliyon*, *8*(6), 1–14. https://doi.org/10.1016/j.heliyon.2022.e09724

Naseef, H. H., & Tulaimat, R. H. (2025). Transesterification and esterification for biodiesel production: A comprehensive review of catalysts and palm oil feedstocks. In *Energy Conversion and Management: X, X*(26), 1-42. https://doi.org/10.1016/j.ecmx.2025.100931

Osman, A. I., Nasr, M., Farghali, M., Rashwan, A. K., Abdelkader, A., Al-Muhtaseb, A. H., Ihara, I., & Rooney, D. W. (2024). Optimizing biodiesel production from waste with computational chemistry, machine learning and policy insights: a review. *Environmental Chemistry Letters*, *22*(3), 1005–1071. https://doi.org/10.1007/s10311-024-01700-y

Permanasari, A. R., Sihombing, R. P., Hidayatulloh, C. Y., Al-Ayubi, S., Fhmi, R. M., Kautsar, M. F. W., & Wibisono, W. (2022). The effec of precipitation pH and temperature of the Mg/Al Hydrotalcite synthesis on the glucose isomerization. *International Journal Applied Technology Research*, *3*(1), 22–35. https://doi.org/10.35313/ijatr.v3i1.55

Prayitno, A., Prasetyo, B., & Sutirtoadi, A. (2020). Synthesis and characteristics of nano calcium oxide from duck eggshells by precipitation method. *Second International Conference on Food and Agriculture 2019*, 1–6. https://doi.org/10.1088/1755-1315/411/1/012033

Putri, D. R., Irwan, M., & Nadir, M. (2024). Pengaruh jenis katalis pada pembuatan biodiesel dari minyak jelantah. *Dalton: Jurnal Pendidikan Kimia dan Ilmu Kimia*, *7*(2), 109–114. http://dx.doi.org/10.31602/dl.v7i2.15158

Ramli, M., Saiful, S., Febriani, F., Amraini, A., Fathurrahmi, F., Shellatina, S., & Zuhra, C. F. (2020). Calcined aceh bovine bone

(*Bos indicus*) intercalated lithium as an inorganic base catalyst for transesterification of castor oil. *Aceh International Journal of Science and Technology*, *9*(1), 22–28. https://doi.org/10.13170/aijst.9.1.16622

Safitri, T. R., & Puryanti, D. (2020). pengaruh konsentrasi nh$_4$oh terhadap ukuran nanopartikel nikel ferit ($NiFe_2O_4$) yang disintesis dengan metode kopresipitasi. *Jurnal Fisika Unand*, *9*(3), 318–322. https://doi.org/10.25077/jfu.9.3.318-322.2020

Shabani, M., & Faraji, G. (2020). Processing and characterization of natural hydroxyapatite powder from bovine bone a. *Journal of Ultrafine Grained and Nanostructured Materials*, *53*(2), 204–209. https://doi.org/10.22059/jufgnsm.2020.02.12

Sunardi, S., Krismawati, E. D., & Mahayana, A. (2020). sintesis dan karakterisasi nanokalsium oksida dari cangkang telur. *ALCHEMY Jurnal Penelitian Kimia*, *16*(2), 250–259. https://doi.org/10.20961/alchemy.16.2.40527.250-259